# Microwave response of DNA in solution: Theory

M. E. Davis* and L. L. VanZandt
*Physics Department, Purdue University, West Lafayette, Indiana 47907*
(Received 8 April 1987)

Recent studies by Edwards, Davis, Swicord, and Saffer have indicated resonant absorption of microwave radiation by DNA in solution. Previous theoretical calculations had indicated that such resonances should be overdamped. We present a more realistic model that provides a parametrization for the overcoming of the overdamping. The refinements include the electrically active nature of the solvent and the binding of the first hydration layer. Our results show that the hydration layer binding is the single most important aspect of the phenomenon. The parametrization indicates that the ability of bound layers to transmit shear must be greatly reduced. This is a behavior that can be qualitatively explained in terms of bond orientation by the structured water and reduced bond density for the DNA-water interface as opposed to corresponding surface in pure water. Conclusive results, however, await a discrete molecular modeling of the hydration layer binding.

## I. INTRODUCTION

Acoustic organ pipe modes have been observed in deoxyribonucleic acid (DNA) fibers and films by Maret, Oldenberg, Winterling, Dransfeld, and Rupprecht[1] as well as Lindsay and Powell.[2] In these dry forms the resonances are expected, there being no strong damping mechanism. The theoretical work of Dorfman and VanZandt[3] indicates, though, that for dissolved DNA these acoustic modes are overdamped by the hydrodynamic coupling. To the contrary, however, has come the recent work of Edwards, Davis, Swicord, and Saffer.[4] Their still controversial results show a series of resonances in the microwave frequency range for a solution of DNA of fixed length. The resonance pattern appears be a series of geometric resonances corresponding to integer half-wavelengths on the entire length of polymer. That is, given the allowed wavelength for the normal modes on the molecule and the frequencies of the resonances, one calculates the speed of sound for a compressional mode in DNA comparable to that measured by Hakim, Lindsay, and Powell.[5]

The Dorfman-VanZandt model assumed an electrically neutral solvent and the typical hydrodynamic no-slip boundary condition at the surface of the molecule. This model predicts the overdamping of the acoustic vibrational modes as a consequence of the large water viscosity. The perfect stick condition must go almost to perfect slip to reduce the damping by the two orders of magnitude separating the theory from the experimental results.

The refinement we present includes realistically modeling the counterions and the primary hydration layer. In our initial investigations[6] we included only the counterions as sources to affect the electric fields and drive the solvent. With ions present the oppositely charged ion cloud around the molecule produces a significant shear force in the solvent. Thus in the perfect slip solution a careful balance of large forces is necessary to match the polymer motion to the solvent. A small mismatch in forces can produce large changes in the motion of the DNA and in its power absorption. So with decoupling of the solvent and ion motions a resonant feature can appear in the power absorption. A very simple model of the hydration layer developed by VanZandt[7] provides for just such a slipping by changing the phase of the coupling between the water and the molecule converting the behavior from damped to elastic.

In this paper we explore the parametrization of this binding upon resonance formation as well as the effects of salt concentration and temperature. Our parametrization indicates the primary hydration layer must have properties significantly different from bulk water for resonances to appear. The variations of salt concentration and temperature are shown to have small effects, except to the extent that they may change the binding of the hydration layer.

It seems that the hydration shell binding is the most important factor in the possibility of resonant absorption. Although the parametrization provides some insight to the mechanism, we are left with unanswered questions which must be pursued in further work. It is almost certain that a fuller understanding awaits a discrete molecular model.

## II. MODEL

There are five elements to this model, the polymer, the primary hydration layer, the continuum water, the ions, and the electromagnetic fields. These elements are coupled mechanically as well as electrically. The couplings oppose the relative motion of the elements with elastic and damped character, but the electric field drives the polymer and the counterions in opposite directions. The charge-density fluctuations and currents act as electrical sources which modify the driving field. In this section we examine the elements and their interrelations.

 

### A. The DNA

Prior lattice-dynamic calculations of this research group[8] provide dispersion relations for relatively dry DNA. A typical spectrum can be seen in Fig. 1. From the frequency scale of this diagram we see that in the frequency range of interest, 1–10 GHz, we are almost at the origin, far from any perceptible dispersion. In this region the motion of the polymer is equivalent to that of an elastic rod. The discrete nature of the base pair structure is averaged out by the long wavelength of these low-frequency acoustic modes. We therefore use an elastic rod for our model of the DNA molecule. To provide the computational advantages of cylindrical symmetry we take the rod to be a straight smooth cylinder. With cylindrical symmetry we can also assume that the charge is spread uniformly over the surface of the polymer.

Dorfman and VanZandt have shown that the grooves produce only a 5% effect on the hydrodynamic solution, so we do not expect this approximation to affect the basic nature of the mechanism. As for ignoring the tertiary structure of the DNA, its inclusion would make the calculation much more difficult without promise of providing any significant alteration of behavior in the relaxed plasmids and straight pieces being studied. Unless the structure is such that it introduces significant new interhelical forces this structure will only affect the strength of the coupling to the various modes.

The normal modes for the molecule are determined by the behavior of the ends of the molecule, but this is the only effect of the ends we consider. We will not consider end modes on the polymer or diffraction effects for the electric fields. For the field calculations we will assume translational invariance. We will discuss the mode coupling in more depth below.

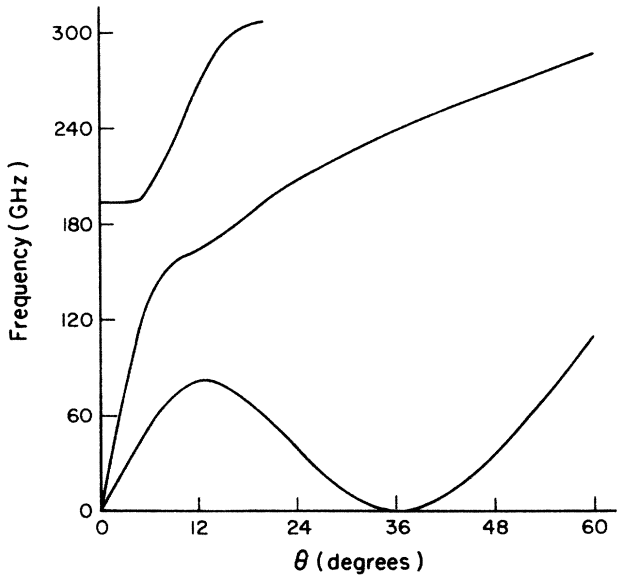


FIG. 1. Low-frequency, low-phase-angle portion of the mode spectrum for relatively dry DNA plotted against the relative phase shift between neighboring base pair motions. The lowest branch is mostly torsional in character near $\theta=0$, changing to bending near the 36° minimum. The second branch is mostly compressional in character in the interesting frequency range. All branches develop complex mixed behavior as frequency and phase angle increase.

To determine the equations of motion for the molecule consider a slice as pictured in Fig. 2. The DNA slice of thickness $dz$ will have mass $\pi r_0^2 \rho_m dz$, or $\Lambda_m dz$, where $\rho_m$ and $\Lambda_m$ are, respectively, the volume and linear mass densities of DNA. Elastic restoring forces will be transmitted to the slice through the flat faces, while the coupling forces of DNA to the hydration layer will be transmitted through the edge of the slice. In addition the surface charge and the ions contained in the hydration layer will respond to the electric field.

Let us consider each of the forces explicitly. Letting $u_m$ be the displacement of the slice from equilibrium, we can write $\Lambda_m c_m^2(\partial^2 u_m/\partial z^2)dz$, for the restoring force, where $c_m$ is the speed of sound in the polymer. The linear charge density $\lambda_m$ is pushed by the electric field at the surface of the molecule, $E_{z0}$ giving a force of $\lambda_m E_{z0} dz$ on the slice. It is assumed that the axial electric field will not vary appreciably over the scale of 1 nm or so. The coupling to the hydration layer is written as a damped interaction $\Gamma$ so this force is given by $\Gamma(v_b - v_m)dz$. This form is still entirely general as an elastic term may be represented as the imaginary part of $\Gamma$.

Adding the forces together gives the equation of motion,

$$\Lambda_m \frac{\partial^2 u_m}{\partial t^2} = \Lambda_m c_m^2 \frac{\partial^2 u_m}{\partial z^2} + \lambda_m E_{z0} + \Gamma(v_b - v_m) . \quad (1)$$

With the compressional waveform of $u = u_m e^{i(kz-\omega t)}$ and noting that $v_m = -i\omega u_m$ we can solve the equation of motion for the velocity of the molecule,

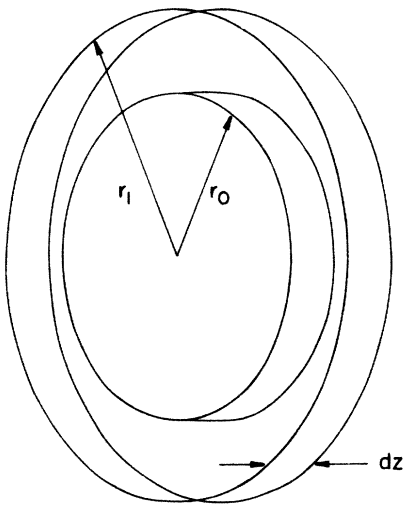


FIG. 2. Polymer slice and nearby water. $r_0$ is the effective radius of the dry polymer; $r_1 - r_0$ is the thickness of the hydration layer, presumably one water molecule thick, hence equal to 0.31 nm. Continuum water surrounds all.

$$v_m = -i\omega \left[ \frac{\lambda_m E_{z0} + \Gamma v_b}{(\omega_0^2 - \omega^2)\Lambda_m - i\omega\Gamma} \right] , \quad (2)$$

where $\omega_0^2 = c_m^2 k^2$.

For numerical values of the DNA constants, we take the specific gravity of the DNA to be 1.5 and the radius of the dry molecule $r_0$ to be $1.0\times10^{-9}$ m. Since the mechanical coupling to the water is incorporated explicitly while the effects of dielectric screening of the long-range forces in the polymer are not, neither the hydrated nor anhydrous DNA velocities are appropriate. Rather, $c_m$ is best represented by the speed of sound measured by Hakim *et al.*[5] for partially hydrated DNA films, or $1.8\times10^3$ m/s. The molecule's linear surface charge density $\lambda_m$ corresponds to a charge of one extra electron per phosphate or $-9.424\times10^{-10}$ C/m.

### B. The primary hydration layer

To determine the equation of motion for the primary hydration layer consider the washer-shaped slice as pictured in Fig. 2. The hydration washer will have mass $\pi(r_1^2 - r_0^2)\rho_b dz$, or $\Lambda_b dz$, where $\rho_b$ and $\Lambda_b$ are, respectively, the volume and linear densities of the hydration layer. Elastic restoring forces will be transmitted to the washer through the flat faces, while the coupling forces of DNA to hydration layer and hydration layer to bulk water will be transmitted through the inside and outside edges, respectively. In addition the ions contained in the layer will respond to the electric field.

Paralleling the development for the molecule we can write $\Lambda_b c_\omega^2(\partial^2 u_b/\partial z^2)dz$ for the elastic restoring forces. As for the electric force, we assume the ions in the hydration layer are locked to the water and directly transmit the force $\lambda_b E_{z0} dz$. $\lambda_b$ is the linear charge density of the ions bound in the first hydration layer. Also, the molecule pushes on the hydration water with a complimentary force, $\Gamma(v_m - v_b)dz$.

The force exerted across any surface element of a continuum fluid is described by the stress tensor. In general the viscous stress tensor $V$ is defined such that the force transmitted across an area $\mathbf{dS} = dS\hat{n}$ is $V\cdot\mathbf{dS}$. For Cartesian coordinates[9]

$$V_{ij} = \eta'\nabla\cdot\mathbf{v}\delta_{ij} + \eta\left[\frac{\partial v_i}{\partial x_j} + \frac{\partial v_j}{\partial x_i}\right] , \quad (3)$$

where $\eta$ is the coefficient of shear viscosity and $\eta'$ is the second or dilational coefficient of viscosity, which is related to $\eta_B$, the bulk or volume viscosity, by $\eta_B = \eta' + \frac{2}{3}\eta$. Being only concerned with the compressional motion of the molecule we want the $z$ component of the force or $\hat{z}\cdot V\cdot\mathbf{dS}$. For the surface we wish to integrate over $\mathbf{dS} = -r_1(\cos\theta\hat{x} + \sin\theta\hat{y})d\theta dz$, so the force on a surface element is given by

$$-r_1(V_{zx}\cos\theta + V_{zy}\sin\theta)d\theta\, dz . \quad (4)$$

Substitution for $V$ yields

$$\eta r_1\left[\left[\frac{\partial v_z}{\partial x} + \frac{\partial v_x}{\partial z}\right]\cos\theta + \left[\frac{\partial v_z}{\partial y} + \frac{\partial v_y}{\partial z}\right]\sin\theta\right]d\theta\, dz . \quad (5)$$

Then converting to cylindrical coordinates, and assuming no $\theta$ dependence of the velocity field, we find the force on our surface element to be

$$\eta r_1 \frac{\partial v_z}{\partial r}(r_1)d\theta\, dz . \quad (6)$$

Finally, integration over $\theta$ introduces a factor of $2\pi$. Thus writing the radial derivative of the axial fluid velocity at the surface as $v'_{z0}$, we have

$$2\pi r_1 \eta v'_{z0} dz \quad (7)$$

as the force from the continuum fluid.

We utilize the small-amplitude approximation to express the time rate of change of momentum as $\pi r_1^2 \rho_m(\partial^2 u_b/\partial t^2)dz$. Gathering all of the terms together we write Newton's second law for the hydration layer,

$$\Lambda_b \frac{\partial^2 u_b}{\partial t^2} = \Lambda_b c_\omega^2 \frac{\partial^2 u_b}{\partial z^2} + \lambda_b E_{z0} + 2\pi r_1 \eta v'_{z0} + \Gamma(v_m - v_b) . \quad (8)$$

As with the equation of motion for the molecule we can solve this expression for the velocity of the DNA after assuming the compressional waveform of $u_b = u_b e^{i(kz-\omega t)}$ and writing the velocities as $-i\omega$ times the displacements,

$$v_m = \left[\frac{\Lambda_b(\omega_1^2 - \omega^2)}{-i\omega\Gamma} + 1\right]v_b - \frac{\lambda_b}{\Gamma}E_{z0} - \frac{2\pi r_1 \eta}{\Gamma}v'_{z0} , \quad (9)$$

where $\omega_1^2 = c_\omega^2 k^2$. We will take no slip hydrodynamic boundary conditions at the bulk-bound water interface, so $v_b = v_{z0}$. This is a second expression for the velocity of the molecule in terms of the continuum fields.

For lack of anything better, we assume that the hydration layer has the same mechanical properties as pure water. That makes the density, $\rho_b$, $1.00\times10^3$ kg/m$^3$ and the speed of sound, $c_\omega$, $1.5\times10^3$ m/s. The radius of the hydration layer $r_1$ we take to be the radius of the polymer plus the mean distance between water molecules for a total of $1.31\times10^{-9}$ m. The ions between $r_0$ and $r_1$ constitute the charge per unit length $\lambda_b$. The calculation of the ion distribution is described below.

We distinguish no other hydration layers because of their shorter relaxation times. Only the primary hydration layer has bonds persisting long enough to be considered on $10^{-10}$ sec time scales. The second hydration layer relaxation times are indistinguishable from bulk water, so we make no such distinction.

### C. The hydration-layer binding

From the analysis of the force transferred across the hydration layer to continuum water interface, we can see that if the DNA were just more water the force per unit length transmitted across the surface at $r_0$ would be

$$2\pi r_0 \eta'_{z0} \,. \tag{10}$$

How is this altered by the fact that DNA is not water? To answer that let us consider the nature of water and viscosity. Viscosity results from the transfer of transverse momentum across a surface. This transfer can happen in two ways. The first and probably more common conception is that fast molecules move from the passing lane and pull the slower traffic along, while slow molecules intermittently jump into the passing lane causing a pileup in the fast lane. This mechanism can only work on time scales large compared to the time a water molecule has for moving around.

A second, and in this case more appropriate, mechanism can transfer momentum even on shorter times. The second mechanism requires a closer look at what water is and is not. It is not just a dense ideal gas. The water molecule on short time scales can be pictured as oscillating about an equilibrium position just as an atom in an elastic solid does. The only difference is that intermittently bonds become broken, the molecules in a given area rearrange, and a new equilibrium is established. This viewpoint is referred to as the *V*-Structure in the literature (see, for example, Eisenberg and Kauzman[10]). Without the movement of the water atoms the transport of transverse momentum is accomplished by this binding structure. Bonds stretch, break, and reform exerting forces on their neighbors in the process.

There is a characteristic time $\tau_1$ associated with this process. For times shorter than this characteristic time the water behaves more as an elastic solid. For longer times the liquid behaves as a viscous fluid. This modeling of the transition by a single relaxation time is called the Maxwell model.[11] The viscosity is expressible as $\eta/(1-i\omega\tau_1)$. For bulk water the characteristic time is of the order of $10^{-12}$ sec, two orders of magnitude smaller than the microwave time scales of interest. Thus bulk water is almost purely viscous. At the molecule, however, the relaxation times for the first two hydration layers have been measured by Tao, Lindsay, and Rupprecht[12] and found to be significantly different from bulk water.

In addition to this viscoelastic change the geometrical orientation of the bonds across the surface will not be identical to those of a surface in bulk water. The bond orientations enter because bonds normal to the interface are stretched less by shearing motion than those more oblique. The viscous force must include an averaging over bond orientations. It is reasonable to believe that bonds across the water-DNA interface will exhibit a different average. The water to polymer bonds are also less numerous than in bulk, so we introduce a further factor $G$ to model these effects,

$$\left[\frac{2\pi r_0 G\eta}{1-i\omega\tau_1}\right]\frac{dv_z}{dr} \,. \tag{11}$$

This is the general form we use for the coupling.

As we are dealing with discrete layers, the molecule and the first hydration layer, the radial derivative becomes $\delta v_z/\delta r$ or $(v_b - v_m)/(r_1 - r_0)$, so we can write the force as

$$\left[\frac{2\pi r_0 G\eta}{(r_1-r_0)(1-i\omega\tau_1)}\right](v_b - v_m) \,. \tag{12}$$

Comparison with the term in Eq. (1) shows that the factor in large parentheses is $\Gamma$.

At this point let us examine our expectations for $G$. First consider the number of bonds that might cross the water-DNA surface as opposed to a water-water surface. In one turn of the double helix there are 20 phosphate groups providing at most 80 oxygen atoms for hydrogen bonding. Kopka, Fratin, Drew, and Dickerson[13] have shown that the esterized oxygens do not participate strongly in hydrogen bonds, which leaves only 40 oxygen atoms. A similar cylindrical shell of water atoms would hold 300 oxygen atoms. As a result, we would expect a factor of 0.13 to be part of $G$.

As for the orientational effects, in Fig. 3 we show the effect of a translational movement of the layers on a given bond. For small displacements the effective translational force constant $f_z$ is given by $f_s \sin^2\theta + f_\theta \cos^2\theta$, where $f_s$ and $f_\theta$ are the stretch and bending force constants, respectively. If these are two water layers we expect all orientations to be equally possible. In this case the average force transmitted by a bond between water-water layers is $\frac{1}{3}f_s + \frac{2}{3}f_\theta$. For a water-DNA interface, on the other hand, the bonds may be constrained more nearly perpendicular to the polymer axis. Then the motion is entirely bending and the average force constant is just the bending force constant. With the stretch force constant being roughly ten times the bending force constant for hydrogen bonds this would introduce another factor of 0.25 into $G$.

Thus with only two very simple considerations a value of 0.03 for $G$ is reasonable. With further considerations, for example, the dependence of hydrogen bond strength

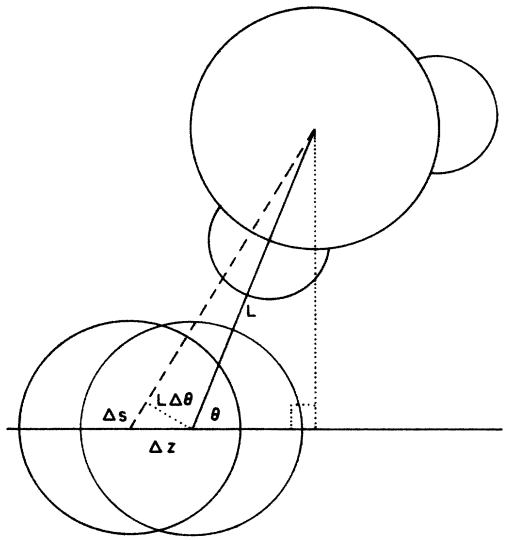


FIG. 3. Hydrogen bond stretching as a result of a relative translation of the participating oxygen atoms. The translation $\Delta z$ results in a combination of stretch $\Delta s$, and angle bend $L\Delta\theta$ dependent on the bond orientation $\theta$.

upon separation[14] or the disruption of hydrogen bonds by the large counterion concentration, this factor could be still smaller. As we shall see, a value of 0.02 produces a good fit to the Edwards, Davis, Saffer, and Swicord (EDSS) data.

### D. The ions

Commonly DNA samples consist of DNA molecules in NaCl solutions. We model our ions accordingly as two species with opposite monovalent charges. For simplicity we choose identical masses as well as identical water coupling constants for the two species. The use of identical masses for the ions introduces only a very small approximation, since in the region where the ion effects are important, i.e., close to the molecule, only the positive ions are actually present in significant quantities. So the mass $m$ is taken as that of a $Na^+$ ion. The use of identical damping constants results in zero solvent velocity in the far bulk liquid.

The behavior of the ions, as well as the electric fields, can be divided into two parts according to the frequency response. The zero frequency or "static" describes the equilibrium distribution of the ions and electric fields when no microwave illumination is present. The microwave frequency or "dynamic" part describes the response to gHz radiation. The dynamic response is a small perturbation on the static system.

In the static case we determine a radially varying number density of each of the species. We can consider this as a continuous number density in the face of the atomic dimensions of the problem because of the disparity between the time scale of the thermal oscillations and that of the microwave excitations. The average time between thermal collisions is of the order of $10^{-13}$ sec, while for microwaves the period is of the order $10^{-9}$ sec. On this time scale the discrete nature becomes a blur and the time-averaged number density is the physically important behavior.

In equilibrium, the ions distribute themselves to balance the electrostatic force with the "pressure" of the concentration gradient. This balance is approximately described by the Poisson-Boltzmann equation, which has been shown by Fixman[15] to be a good approximation for small bulk salt concentrations. The basic equation arises from combining Poisson's equation for the electrostatic potential $\phi$,

$$\epsilon_{dc}\nabla^2\phi = -e(n_+ - n_-) , \tag{13}$$

with the assumption that the number densities have a Boltzmann dependence on electric potential,

$$n_\pm = n_\infty e^{\mp e\phi/k_B T} , \tag{14}$$

where $\epsilon_{dc}$ is the dc permittivity of the solvent, $n_\pm$ are the positive and negative ion number densities, $n_\infty$ is the bulk ion number density, $k_B$ is the Boltzmann constant, and $T$ is the temperature. These expressions are then numerically integrated to obtain $n_+$ and $n_-$ for use in the dynamic calculation.

The dynamic case describes the coupling of this equilibrium distribution to the electromagnetic fields and the solvent motion. The force on the ions from the electromagnetic fields would in general have two terms, $\mathbf{E}$ and $\mathbf{v}\times\mathbf{B}$, but the $\mathbf{v}\times\mathbf{B}$ term is of second order in the disturbance. So, in keeping with the harmonic approximation assumed for the molecule, we neglect this term and consider the ions to be only driven by the electric field. As for the coupling of the solvent and the ions, the force between them is assumed proportional to the relative velocity with a proportionality constant $\tau$ chosen to produce the proper dc resistance. Typical values for $\tau$ are of the order $10^{-14}$ sec, indicating that the ions are very strongly locked to the motion of the liquid as far as our microwave time scales are concerned. With the forces well in hand and neglecting the nonlinear term $m\mathbf{v}_\pm(\partial n_\pm/\partial t)$, we can now write out Newton's second law for the ion densities

$$n_\pm m\frac{\partial \mathbf{v}_\pm}{\partial t} = \pm n_\pm e\mathbf{E} + \frac{n_\pm m}{\tau}(\mathbf{v}-\mathbf{v}_\pm) , \tag{15}$$

where $\mathbf{v}_\pm$ are the velocities of the positive and negative ions and $\mathbf{v}$ is the velocity of the fluid.

Finally, an $e^{-i\omega t}$ time dependence allows us to express the ion velocities in terms of the electric fields and the solvent velocity,

$$\mathbf{v}_\pm = \frac{\pm(e\tau/m)\mathbf{E}+\mathbf{v}}{1-i\omega\tau} . \tag{16}$$

This expression will enable us to replace the ion velocities in the calculation.

As stated previously the ions are modeled as primarily $Na^+$ ions. The monovalent ionic charge $e$ is $\pm 1.602\times10^{-19}$ C while $3.8\times10^{-26}$ kg is used for the mass $m$. The dc permittivity of water is $7.08\times10^{-10}$ $C^2/J\,m$. Finally, the damping constant is chosen to match the dc conductivity. We obtain this relation by solving for the steady state of the equation of motion for the ions. For a homogeneous salt solution our choice of identical masses and coupling constants for the ions species results in zero net force on the solvent, resulting in no net solvent velocity. In this case Newton's second law for the ions reduces to two terms: the electric driving term and the damping term. Solving for the current density we find the conductivity as the coefficient of the electric field $\sigma = 2e^2 n_\infty \tau/m$. We use a value of $1.0\times10^{-2}$ mho/m for a 5-mM salt solution. So, the value of $\tau$ is $2.48\times10^{-14}$ sec. This indicates the ions are strongly glued to the solvent on microwave time scales. The value of the conductivity for a 5-mM NaCl solution should be $5.0\times10^{-3}$ mho/m, which would lock the ions even more tightly to the solvent. The value of $\tau$ we use does not impact significantly on the dynamics for we shall see that they depend solely upon $(1-i\omega\tau)$. This is effectively unity at gHz frequencies. The only noticeable change using the correct value for $\tau$ is a factor of 2 reduction in the small constant ion absorption.

### E. The solvent

The solvent surrounding the DNA molecule and hydration layer is modeled as a viscous inertial continuum, as done by Dorfman and VanZandt. The inclusion of

the ions, however, introduces a driving force internal to the fluid in addition to the solvent-molecule boundary force of the Dorman-VanZandt model. As with the ions the disparity between thermal collision times and the time scale of interest allows the continuum representation to be used on a system of molecular dimensions. Nonlinear behavior is neglected because of the small amplitude of the oscillations in consideration. The maximum velocities found in our calculations are $\sim 10^{-3}$ m/sec, which corresponds to a Mach number of $\sim 10^{-6}$. This approximation is also consistent with the harmonic approximation used for the molecule itself.

The equation of motion for a viscous inertial continuum is the Navier-Stokes equation,[9] Newton's second law applied to a classical continuum,

$$\eta_0 \nabla(\nabla\cdot\mathbf{v}) - \eta \nabla\times\nabla\times\mathbf{v} + \mathbf{F} - \nabla P = \frac{D(\rho_\omega \mathbf{v})}{Dt} \ . \tag{17}$$

As used previously, $\mathbf{v}$ is the velocity field of the fluid. The new fields $\mathbf{F}$ and $P$ are, respectively, the force density exerted on the water by the ions and the pressure. The other constants characterize the water with $\rho_\omega$ being the mass density of the water and $\eta$ being the viscosities. Following the naming convention found in the *American Institute of Physics Handbook*,[9] $\eta$ is the shear viscosity coefficient and $\eta_B$ is the bulk or volume viscosity coefficient. $\eta_0$ is a local contraction for $\eta$ times the viscosity number or $\eta_B + \frac{4}{3}\eta$.

As we stated above we ignore the second-order terms arising in the total time derivative because of the small amplitudes involved. Specifically the terms $\rho_\omega(\mathbf{v}\cdot\nabla)\mathbf{v}$ and $\mathbf{v}(\partial\rho_\omega/\partial t)$ are dropped. The pressure term is expressed in terms of the velocity of the water through the equation of state,

$$\frac{\partial P}{\partial t} = -c_\omega^2 \rho_\omega \nabla\cdot\mathbf{v} \ , \tag{18}$$

where $c_\omega$ is the speed of sound in the water. The force term $\mathbf{F}$ results from the coupling between the ions and the water. Therefore, it must be equal and opposite to the force of the liquid on the ions,

$$\mathbf{F} = [n_+(\mathbf{v}_+ - \mathbf{v}) + n_-(\mathbf{v}_- - \mathbf{v})]\frac{m}{\tau} \ . \tag{19}$$

So, assuming a time dependence of $e^{-i\omega t}$, we can eliminate $\mathbf{F}$ and $P$ from the Navier-Stokes equation to obtain

$$\eta_1 \nabla(\nabla\cdot\mathbf{v}) - \eta \nabla\times\nabla\times\mathbf{v} + [n_+(\mathbf{v}_+ - \mathbf{v}) + n_-(\mathbf{v}_- - \mathbf{v})]\frac{m}{\tau} = -i\omega\rho_\omega \mathbf{v} \ , \tag{20}$$

where $\eta_1 \equiv \eta_0 - (c_\omega^2 \rho_\omega / i\omega)$.

The numerical values for the solvent are taken to be typical values for distilled water. The speed of sound $c_\omega$ is taken to be $1.5\times 10^3$ m/s. The viscosities are obtained from Eisenberg and Kauzman[10] who give them as 0.01 Poise for the shear viscosity $\eta$ and $3\eta$ for the volume viscosity $\eta_B$. The density $\rho_\omega$ is $1.0\times 10^3$ kg/m$^3$.

### F. The electric fields

The driving agent for this system is the rf electric field. The microwave electric fields produce currents and charge densities that in turn modify the fields themselves. This behavior is described by Maxwell's equations with no approximations. The counterion density fluctuations and velocities comprise the field sources in the solvent. Similarly, the compressional fluctuations in the polymer and hydration layer act as sources which determine the fields at the hydrated molecule-continuum interface.

Let us consider Maxwell's equations in the fluid

$$\nabla\times\mathbf{E} = \frac{\partial \mathbf{B}}{\partial t} \ , \tag{21}$$

$$\frac{1}{\mu_0}\nabla\times\mathbf{B} = e(n_+\mathbf{v}_+ - n_-\mathbf{v}_-) + \epsilon_\omega \frac{\partial \mathbf{E}}{\partial t} \ , \tag{22}$$

$$\epsilon_\omega \nabla\cdot\mathbf{E} = e(\Delta n_+ - \Delta n_-) \ , \tag{23}$$

$$\nabla\cdot\mathbf{B} = 0 \ . \tag{24}$$

Assuming a time behavior of $e^{-i\omega t}$ we can eliminate $\mathbf{B}$ by combining the Ampere and Faraday laws,

$$\nabla\times\nabla\times\mathbf{E} = i\omega\mu_0[e(n_+\mathbf{v}_+ - n_-\mathbf{v}) - i\omega\epsilon_\omega \mathbf{E}] \ . \tag{25}$$

Gauss's law on the electric fields just defines the charge conservation formula that is expected for the charge-density fluctuations, $\nabla\cdot n_\pm = -\partial\Delta n_\pm/\partial t$. To put it another way, substitution of this form into Gauss's law yields the divergence of the Ampere-Faraday law,

$$0 = \nabla\cdot[e(n_+\mathbf{v}_+ - n_-\mathbf{v}_+) - i\omega\epsilon_\omega \mathbf{E}] \ . \tag{26}$$

So if we satisfy the Ampere-Faraday law then Gauss's law will automatically follow. Gauss's law for the magnetic fields is also automatic. This results from the $e^{-i\omega t}$ time dependence and the lack of a monopole term in Faraday's law, for in this case $\mathbf{B}$ is proportional to the curl of $\mathbf{E}$. The divergence of a curl always being zero, Gauss's law for the magnetic fields is guaranteed.

Just as the equations of motion became boundary conditions for the fields in the continuum solvent, Maxwell's equations applied to the polymer and its shell will relate the motion of the DNA to the surrounding fields. Ampere's law for the hydrated molecule is more convenient in its integrated form, but Gauss's laws still follow from the Ampere's and Faraday's laws. Ampere's law over a cross section of the molecule states

$$\frac{1}{\mu_0}\int_0^{2\pi} B_\theta r_1 \, d\theta = \lambda_m v_m + \lambda_b v_b - i\omega \int_0^{2\pi}\int_0^{r_1} \epsilon E_z r \, dr \, d\theta \ . \tag{27}$$

The integrations are straightforward. Cylindrical symmetry allows us to integrate over $\theta$. Then, as we assumed when writing out the equations of motion for the hydrated molecule, we take the axial electric field to be constant over the cross section of the molecule. This allows us to also do the radial integration, noting the change in dielectric constant at $r_0$. Finally we solve for $v_m$,

$$v_m=\frac{1}{\lambda_m}\left[-\lambda_b v_b+i\omega\pi[\epsilon_m r_0^2+\epsilon_\omega(r_1^2-r_0^2)]E_{z0}+\frac{2\pi r_1}{\mu_0}B_\theta\right] . \quad (28)$$

Thus we have a third expression tying the DNA motion to the continuum fields.

For the permittivity of the polymer $\epsilon_m$ we use a constant $4.427\times10^{-11}$ C$^2$/J m independent of frequency. On the other hand, because of the large dielectric absorption of microwaves by water and the availability of data, $\epsilon_\omega$, the water permittivity, is given by

$$\epsilon_\omega=\frac{\epsilon_{dc}-\epsilon_\infty}{1-i\omega\tau_D}+\epsilon_\infty . \quad (29)$$

From Eisenberg and Kauzman[10] we obtain the values of the dc and optic dielectric constants and the dielectric relaxation time. These translate to $7.08\times10^{-10}$ C$^2$/J m for $\epsilon_{dc}$, $8.85\times10^{-11}$ C$^2$/J m for $\epsilon_\infty$, and $1.0\times10^{-11}$ sec for $\tau_D$.

### G. The modes

The most uncertain step of our calculation is the proper connection of the millimeter wavelength driving field to the micrometer wavelength disturbances on the molecule. The microwave illumination is effectively uniform over the region of the molecule, while the acoustic waves on the molecule and the response waves have wavelengths on the order of the molecule size.

To address the special complexities of this difficulty first let us examine a case where the connection is simple. Let us consider a charged elastic rod driven directly by a uniform electric field $E_0e^{-i\omega t}$. The equation of motion is

$$m\frac{\partial^2 u}{\partial t^2}=mc^2\frac{\partial^2 u}{\partial z^2}+\lambda E_0e^{-i\omega t}-\gamma\frac{\partial u}{\partial t} . \quad (30)$$

The general steady-state solution is of the form

$$u=[u_s+a\cos(k_sz)+b\sin(k_sz)]e^{-i\omega t} , \quad (31)$$

where $k_s^2=(\omega^2-i\omega\gamma/m)/c^2$ and $u_s=\lambda E/(m\omega^2+i\omega\gamma)$. The coefficients $a$ and $b$ are determined by the boundary conditions at the end of the rod.

In the case of fixed ends at $z=-L/2$ and $z=L/2$ the solution is

$$u=u_s\left[\frac{\cos(k_sz)}{\cos(k_sL/2)}-1\right] . \quad (32)$$

Decomposing this into a Fourier series in the normal modes of the rod, we obtain the series

$$u=\frac{4u_sk_s^2}{L}\sum_{n=0}^{\infty}\frac{(-1)^n\cos(k_nz)}{k_n(k_n^2-k_s^2)} , \quad (33)$$

where $k_n=(2n+1)\pi/L$.

Compare this result with one obtained by assuming an infinite rod driven by a stepped electric field. In this latter situation, we expand the electric field in a Fourier series

$$E=\frac{4E_0}{L}\sum_{n=0}^{\infty}\frac{(-1)^n\cos(k_nz)}{k_n} . \quad (34)$$

The displacement $u$ is similarly expanded with unknown coefficients. The linear independence of the $\cos k_nz$ functions requires the equation of motion to hold term by term,

$$-m\omega^2u_n=-mc^2k_n^2u_n+\frac{4\lambda E_0(-1)^n}{k_nL}+i\omega\gamma u_n . \quad (35)$$

The culmination of this process is

$$u=\frac{4u_sk_s^2}{L}\sum_{n=0}^{\infty}\frac{(-1)^n\cos(k_nz)}{k_n(k_n^2-k_s^2)} , \quad (36)$$

which is an extremely comparable result.

In the case of free ends the molecule moves as a rigid whole and both $a$ and $b$ are zero. The motion is now identical to an infinite rod in a constant field. For the more realistic case though, where the rod's ends are somewhere between free and fixed, it can be shown that the solution is comparable to a constant field plus a stepped field. The amplitude of the driving field for each mode on the infinite rod is a measure of the coupling of the driving field to that mode. In addition to the end conditions the real geometry of the molecule affects the coupling. Bending will reduce the coupling to the lower harmonics, and allow coupling to the even and higher harmonics. So we have found one of the nontrivial difficulties in our system.

The problem we are faced with has an additional complication: The electric field is not simply uniform. The transit through the finite length ion cloud and the acoustic wavelength charge perturbations produce short-wavelength adjustments to the electric field. The expansion of the electric fields in terms of the normal modes of the molecule looks like a promising alternative. The second problem, however, is that by introducing the $e^{ikz}$ dependence we change the radial dependence of the asymptotic electric fields as well.

If we had an infinite length molecule in an infinite length field we would just have a scattering problem where we would decompose the electromagnetic plane wave as

$$e^{iqx}=\sum_{l=0}^{\infty}\frac{i^l}{q}J_l(qr)\cos(l\theta) , \quad (37)$$

where $q$ is $2\pi/\lambda_{\text{microwave}}$. The only field that is nonzero at the small radius of the molecule is the $l=0$ wave. The Bessel functions of the first kind, $J_l$, behave asymptotically as $(1/\sqrt{r})\sin(qx)$. This is the form of a cylindrical standing wave or a sum of incoming and outgoing waves. These outgoing and incoming waves are the Hankel functions $H_l^{(1)}$ and $H_l^{(2)}$.

As we will show when we derive the asymptotic solutions for the fields, however, the radial dependence of the electric fields with $e^{ikz}$ axial behavior is not $J_0(qr)$ but $J_0(q'r)$, where $q'$ is actually much closer to $k$ than to

$q$. The plane-wave expansion does not work with these $J_l(q'r)$ basis functions. We should expect this because an exact decomposition would require accounting for diffraction effects at the ends of the molecule. It is still meaningful to say that the relative amplitudes are measures of the coupling to that mode.

So we can assign relative amplitudes to each of the modes as seems appropriate for the geometry. We still need a relation from these relative amplitudes to the amplitude being produced by the microwave source. To provide a relationship we calculate the power absorbed in a solution without DNA using the same modes and driving amplitudes. This should sum to $\frac{1}{2}E_s^2[\sigma+\mathcal{R}(-i\omega\epsilon_\omega)]\pi r_{\max}^2$, where $E_s$ is the source field amplitude. Thus we obtain our field calibration.

## III. STATIC CALCULATION AND RESULTS

The calculation of the equilibrium distribution of the ions not only provides the distributions needed by the calculation of the dynamic problem, but also sets the mesh in the radial direction. Starting from the molecule the calculation steps outward using an Euler predictor corrector algorithm.[16] The size of the radial steps is chosen by the algorithm to change the value of $n_+$ by about 0.5% of its original value per step as the integration proceeds from the molecule. With this procedure the step size increases with radius. For the dynamic calculation there must be a cap put on this progression. The program achieves this by fixing the step size once it has grown large enough to fill out the rest of the array and just reach the desired maximum radius. The maximum radius is chosen to produce a system that is 0.1% DNA by volume.

In Fig. 4 we present a typical positive-ion distribution. This distribution is for a $5\times10^{-3}$ molar NaCl solution at a temperature of 298 K. The inset on Fig. 4 shows a close up of this distribution near the hydration-layer–bulk-water interface. Individual points show the graininess of the mesh.

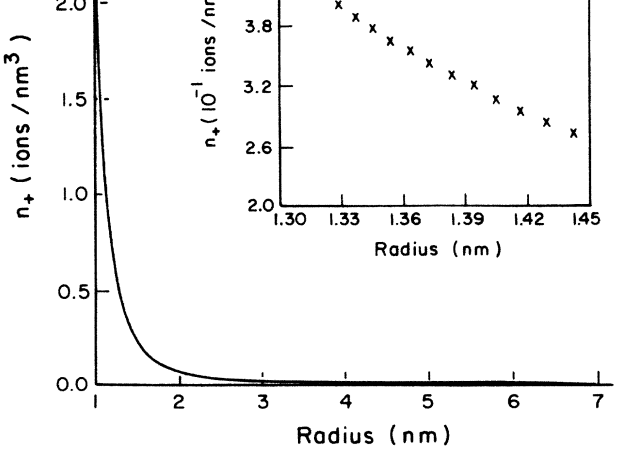


FIG. 4. Positive-ion number density vs radial distance from the DNA axis for a 5-mm bulk salt solution at 298 K. Inset shows closeup of the mesh just outside of the primary hydration layer.

The ion distributions depend only upon the temperature and the bulk salt concentration. With increasing temperature the ion distribution shifts outward, decreasing the salt concentration close to the molecule. The behavior with respect to bulk salt concentration is best understood in terms of the Manning condensation model as examined by LeBret and Zimm.[17] There is a radius at which the fractional amount of charge neutralization of the DNA by the counterion cloud is independent of bulk salt concentration. Outside this radius the neutralizing charge moves outward with decreasing bulk salt, while inside it a decrease in bulk salt causes the neutralizing charge to constrict about the molecule.

## IV. DYNAMIC CALCULATION

Our model for the DNA-ionic solvent system mathematically involves a set of linear differential equations that describe the interrelations of the solvent velocity field, the ion velocity fields, and the electric fields. This system of equations is supplemented by the boundary conditions, which at infinity represent the illuminating microwave field and at the molecule surface represent the motion of the hydrated polymer as it couples to these fields.

We integrate the fields inward from their asymptotic forms and match the boundary conditions at the surface. This requires adjusting the amplitudes of the asymptotic forms until all of the boundary conditions are met. Then once the dynamics of the system are known, we can easily calculate the power that is being drawn from the electric fields by all of the system as $\frac{1}{2}\mathcal{R}\int(\mathbf{E}^*\cdot\mathbf{J})d\tau$.

### A. Combining equations

In this section we reduce the vector equations to scalar equations. Substituting $\mathbf{v}_\pm$ from Eq. (16) into the Ampere-Faraday law and the Navier-Stokes equation, we obtain two coupled vector differential equations in the solvent velocity and the electric fields,

$$\eta_1\nabla(\nabla\cdot\mathbf{v})-\eta\nabla\times\nabla\times\mathbf{v}+i\omega(\rho_\omega+mN_+)\mathbf{v}=-eN_-\mathbf{E}\ , \tag{38}$$

$$\nabla\times\nabla\times\mathbf{E}-\omega^2\mu_0\epsilon_\omega\left[1+\frac{i\tau e^2N_+}{\omega m\epsilon_\omega}\right]\mathbf{E}=i\omega\mu_0eN_-\mathbf{v}\ . \tag{39}$$

In these expressions we have defined $N_\pm\equiv(n_+\pm n_-)/(1-i\omega\tau)$.

From cylindrical symmetry we know the longitudinal waveforms for the electric and velocity fields to be

$$\mathbf{E}=[E_r(r)\hat{r}+E_z(r)\hat{z}]e^{ikz} \tag{40}$$

and

$$\mathbf{v}=[v_r(r)\hat{r}+v_z(r)\hat{z}]e^{ikz}\ . \tag{41}$$

Substitution into the Navier-Stokes equation yields

$$\frac{\eta}{r}\frac{d}{dr}\left[r\frac{dv_z}{dr}\right]+(i\omega M-\eta_1 k^2)v_z = ik(\eta-\eta_1)\frac{1}{r}\frac{d(rv_r)}{dr}-eN_-E_z \quad (42)$$

for the $z$ component, while the $r$ component is

$$\eta_1\frac{d}{dr}\left[\frac{1}{r}\frac{d(rv_r)}{dr}\right]+(i\omega M-\eta k^2)v_r = ik(\eta-\eta_1)\frac{dv_z}{dr}-eN_-E_r\ , \quad (43)$$

where $M\equiv\rho_\omega+mN_+$. Similarly we can write the component equations of the Ampere-Faraday equation. The $z$ component becomes

$$\frac{1}{r}\frac{d}{dr}\left[r\frac{dE_z}{dr}\right]+K^2E_z=ik\frac{1}{r}\frac{d(rE_r)}{dr}-i\omega\mu_0 eN_-v_z\ , \quad (44)$$

and the $r$ component

$$(K^2-k^2)E_r=ik\frac{dE_z}{dr}-i\omega\mu_0 eN_-v_r\ , \quad (45)$$

where

$$K^2\equiv\omega^2\mu_0\epsilon_\omega\left[1+\frac{ie^2\tau N_+}{m\omega\epsilon_\omega}\right].$$

Equation (45) can now be utilized to eliminate $E_r$ from the system of equations without increasing the order of the equations. Thus we obtain a system of three coupled scalar second-order differential equations for the solvent velocity and the axial electric field.

### B. The asymptotic solutions

The boundary conditions at large distances from the molecule are quite simple conceptually. The fluid velocity must vanish at large distances. In the uniform salt solution the force from the positive-ion motion cancels the force from the negative-ion motion leaving no net driving force on the water. At large distances the electric field does not vanish but must represent the microwave illumination.

The asymptotic solutions represent incoming and outgoing waves. So we satisfy the first condition by requiring that asymptotically the fluid velocity be an outgoing wave. The electric field, on the other hand, has both an incoming and outgoing wave just as we discussed previously. The incoming wave has a fixed amplitude representing the microwave illumination coupling to this mode. The outgoing wave is the illumination modified by scattering.

To integrate these equations in from large distances we must know the asymptotic forms of the solutions. To this end we note that the electric fields and the velocity fields couple through differences in the ion concentrations. This difference vanishes at large distances faster than exponentially. As a result at large distances the differential equations reduce to Bessel's equation with complex arguments,

$$v_r''+\frac{1}{r}v_r'+\left[\frac{i\omega M_\infty-k^2\eta}{\eta_1}-\frac{1}{r^2}\right]v_r=-ik\left[1-\frac{\eta}{\eta_1}\right]v_z'\ , \quad (46)$$

$$v_z''+\frac{1}{r}v_z'+\frac{i\omega M_\infty-k^2\eta_1}{\eta}v_z=ik\left[1-\frac{\eta_1}{\eta}\right]\left[v_r'+\frac{1}{r}v_r\right], \quad (47)$$

$$E_z''+\frac{1}{r}E_z'+\kappa_e^2E_z=0\ . \quad (48)$$

For brevity we have defined

$$M_\infty\equiv\rho_m+\frac{2mn_\infty}{1-i\omega\tau}\ ,$$

as well as $\kappa_e^2\equiv K^2-k^2$.

The equation for the electric fields becomes a single equation in the axial electric field, which has two independent solutions. So the asymptotic expression for the electric field is the sum of the incoming driving field and the outgoing response field or

$$E_z(\text{asym})=a_1H_0^{(1)}(\kappa_e r)+E_0H_0^{(1)}(-\kappa_e r)\ , \quad (49)$$

where the $H_0$ represents Hankel functions of the first kind. [Note that $H_0^{(1)}(-z)=H_0^{(2)}(z)$.]

The component equations from the Navier-Stokes equation become two Bessel's equations coupled by an inhomogeneous term in the other component. The form of the solution can be anticipated when one notes the recurrence relations

$$H_0'(x)=-H_1(x)\ , \quad (50)$$

$$H_1'(x)+\frac{1}{r}H_1=H_0(x)\ . \quad (51)$$

The homogeneous equations have for $v_r$ a Bessel function of order 1 and for $v_z$ a Bessel function of order 0. The inhomogeneous terms couple to this reducing the first order to zeroth and the zeroth order to first. Substitution of the forms $b_zH_0(\kappa_v r)$ and $b_rH_1(\kappa_v r)$ for $v_z$ and $v_r$, respectively, yields the expressions

$$b_r\left[\frac{i\omega M_\infty-\eta k^2}{\eta_1}-\kappa_v^2\right]=-ik\left[\frac{\eta}{\eta_1}-1\right]\kappa_v b_z\ , \quad (52)$$

$$b_z\left[\frac{i\omega M_\infty-\eta_1 k^2}{\eta}-\kappa_v^2\right]=ik\left[1-\frac{\eta_1}{\eta}\right]\kappa_v b_r\ . \quad (53)$$

There are two values of $\kappa_v^2$ that satisfy these equations. They correspond to compression and shear waves

$$\kappa_{v1}^2=\frac{i\omega M_\infty}{\eta_1}-k^2\ , \quad (54)$$

$$\kappa_{v2}^2=\frac{i\omega M_\infty}{\eta}-k^2\ . \quad (55)$$

For each of these $\kappa$'s a specific ratio of the amplitudes is

required. For the $\kappa_{v1}$ solution

$$\frac{b_{r1}}{b_{z1}}=\frac{i\kappa_{v1}}{k} , \tag{56}$$

while for the $\kappa_{v2}$ solution

$$\frac{b_{r2}}{b_{z2}}=\frac{k}{i\kappa_{v2}} . \tag{57}$$

Since all of the velocity fields must vanish at infinity we keep only the outwardly decaying modes. The general asymptotic solution is then

$$v_z(\text{asym})=b_{z1}H_0^{(1)}(\kappa_{v1}r)+b_{z2}H_0^{(1)}(\kappa_{v2}r) , \tag{58}$$

$$v_r(\text{asym})=\frac{b_{z1}i\kappa_{v1}}{k}H_1^{(1)}(\kappa_{v1}r)+\frac{b_{z2}k}{i\kappa_{v2}}H_1^{(1)}(\kappa_{v2}r) , \tag{59}$$

$$E_z(\text{asym})=a_1H_0^{(1)}(\kappa_e r)+E_0H_0^{(1)}(-\kappa_e r) . \tag{60}$$

With these forms elucidated a choice for the three unknown amplitudes determines the fields and derivatives at a given radius. This is all of the information necessary to prime the Euler predictor corrector algorithm for the second-order equations. So, given the three complex amplitudes, the fields can be integrated to the molecule. The boundary conditions at the molecule determine the correct amplitudes.

### C. The boundary conditions

At the surface of the hydrated molecule we need three boundary conditions to determine the continuum fields. Requiring that the solvent not penetrate the molecule is the most straightforward of these. This is accomplished by requiring the radial component of the solvent velocity to vanish at the outer surface of the hydrated polymer. The small molecule radius relative to the acoustic wavelengths indicates that the radial velocity would not be significant at $r_1$, even if the molecule were not present. The choice of perfect radial rigidity simplifies the equations for the hydrated molecule without seriously departing from its actual space-filling behavior.

The other two conditions, on the other hand, are consistency conditions. They arise from matching the three distinct mechanisms tying the motion of the molecule to the velocity and electric fields in the solvent. We express this by requiring the equation of motion for the molecule, Eq. (2), the equation of motion for the hydration layer, Eq. (9), and Ampere's law around the hydration layer, Eq. (28), to all consistently predict the velocity of the molecule. So we have three nonlinear functions of the three asymptotic amplitudes: $v_r$ at $r_1$ and two independent differences between the three DNA velocity predictions. The simultaneous root of these functions is the physical solution for the fields. A Newton-Raphson technique[16] utilizing a numerical partial derivative is used to find the simultaneous root of this system.

### D. Power absorbed

With the dynamics of the system determined we can calculate the power absorbed from the electric fields. The time-averaged rate of work density done by the harmonic electric fields is $\mathcal{R}(\mathbf{E}_e^*\cdot\mathbf{J})/2$, where $\mathbf{J}(r)$ is the net current density at r. Thus the power absorbed in the DNA molecule per unit length is

$$P_{\text{DNA}}=\mathcal{R}[(\lambda_m v_m-i\omega\epsilon_m E_{z0})E_{z0}^*]/2 . \tag{61}$$

Similarly that absorbed in the hydration layer is

$$P_{\text{hyd}}=\mathcal{R}[(\lambda_b v_m-i\omega\epsilon_\omega E_{z0})E_z(r_0)]/2 . \tag{62}$$

In the continuum we must integrate radially. The ion currents absorb

$$P_{\text{ion}}=\int_{r_1}^{r_{\max}}\mathcal{R}[e(n_+\mathbf{v}_+-n_-\mathbf{v}_-)\cdot\mathbf{E}^*]\pi r\,dr \tag{63}$$

per unit length while the dielectric absorption of the solvent is

$$P_{\text{sol}}=\int_{r_0}^{r_{\max}}\mathcal{R}(-i\omega\epsilon_\omega\mathbf{E}\cdot\mathbf{E}^*)\pi r\,dr . \tag{64}$$

Addition of these individual parts yields the power absorption for the given frequency and mode that has been calculated. Finally, summation over the modes yields the power absorption at a given frequency and repetition at frequency intervals yields a power spectrum. We then subtract a background of the form $a\mathcal{R}(i\omega\epsilon_\omega)+b$, where $a$ is chosen to match $P_{\text{sol}}$ off resonance and $b$ to match $P_{\text{ion}}$ off resonance.

The difficulty now, as we mentioned in the section on modes, is relating the mode amplitudes to the magnitude of the source field. To provide such a connection we calculate the power absorbed in the same geometry but in the absence of DNA. With no DNA present the ion concentrations are homogeneous and the asymptotic solutions are exact everywhere. In this situation the condition that the fields be finite at $r=0$ requires

$$E_z=\sum_{n=0}^{\infty}E_{0n}J_0(\kappa_{en}r) , \tag{65}$$

$$E_r=\sum_{n=0}^{\infty}E_{0n}a_nJ_1(\kappa_{en}r) , \tag{66}$$

where

$$a_n=\frac{-ik_n\kappa_{en}}{k_n^2-\omega^2\mu\epsilon_\omega+\dfrac{2n_\infty e^2\mu}{m(1-1/i\omega\tau)}} . \tag{67}$$

The power per unit length would then be found analytically. We equate this with assuming there is just a uniform field $E_s$ defined such that

$$P_{\text{none}}=\tfrac{1}{2}E_s^2[\sigma+\mathcal{R}(-i\omega\epsilon_\omega)]\pi r_{\max}^2 . \tag{68}$$

Through this we estimate that for all of the absorptions we quote in this paper the source electric field $E_s$ is $6.5\times10^2$ V/m. Because of the linearity of the equations all of the results scale with this number. The fields scale linearly and the powers quadratically.

Although we quote powers as power absorbed per unit length of polymer this can be converted to absorbed power densities as needed. The maximum radius $r_{\max}$ is chosen to make the DNA volume 0.1% of the total

volume, $r^2_{max}=1000r^2_0$. This allows for a conversion to average power densities in this 0.1% volume DNA solution by dividing the power per unit length values by $\pi r^2_{max}$ or $3.14\times10^{-15}$ m$^2$.

## V. DYNAMIC RESULTS

To study the parametrization of the hydration layer we concentrate on modeling a solution 0.1% volume DNA and 5-mm NaCl at 298 K. Since our model applies most accurately to straight molecules we include odd modes from 1 to 17 on a 2700-bp molecule 918 nm long. $1.0\times10^2$ V/m is used for the incoming axial electric field amplitude $E_0$ for each mode and the boundary conditions are required to be met to less than 0.01%.

Using the Tao and Lindsay[12] room temperature value of $3.9\times10^{-11}$ sec for $\tau_1$, we calculate the power spectra for various values of $G$. In Fig. 5 we present the total power minus background absorbed per meter of DNA for a range of values of $G$. The damping causes a broadening and a shifting of the resonances. We see that with decreasing damping the resonances arise first at the high-frequency end of our range and shift progressively toward their undamped locations. At the same time they decrease in width.

Tao and Lindsay present some indications that the relaxation time may be larger. So we generate similar graphs that can be generated for various values of $\tau_1$ at room temperature. Figures 6 and 7 show the shift of the resonances for $\tau_1$ of $1.83\times10^{-10}$ sec and $1.00\times10^{-9}$ sec.

As one would expect there are two ways to decrease the coupling given two parameters: decreasing $G$ and increasing $\tau_1$. The two methods are not identical. A decrease in $G$ decreases both the damping and the stiffening of the molecule while an increase in $\tau_1$ shifts the damping to stiffening. So it is both the width and positions of the resonances which determine $G$ and $\tau_1$, while the resonance heights determine the amplitudes for each mode. Choices of $G$ and $\tau_1$ that keep $G/\tau_1$ roughly constant produce similar positions, but the line widths get smaller with increasing $G$ and $\tau_1$. It is important to note at this point that although there is a large range of spectra that can be fit with this many parameters the field is not limitless. The positions and widths of all the resonances are set by the choice of $G$ and $\tau_1$ and this parametrization always implies that the lowest resonances will be pulled upward in frequency more than the higher ones. This compression of the lowest modes is a major feature of the model.

Let us examine in more detail a particular combination of $G$ and $\tau_1$ that compares well with the results

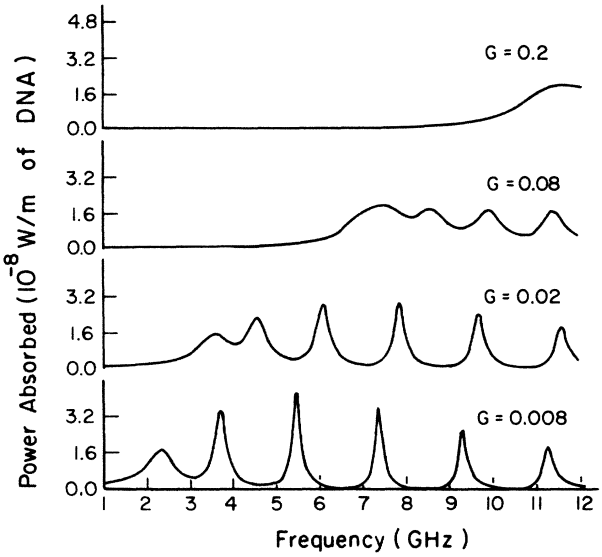


FIG. 6. Background subtracted power absorption spectra for various $G$ values at $\tau_1=0.183$ ns.

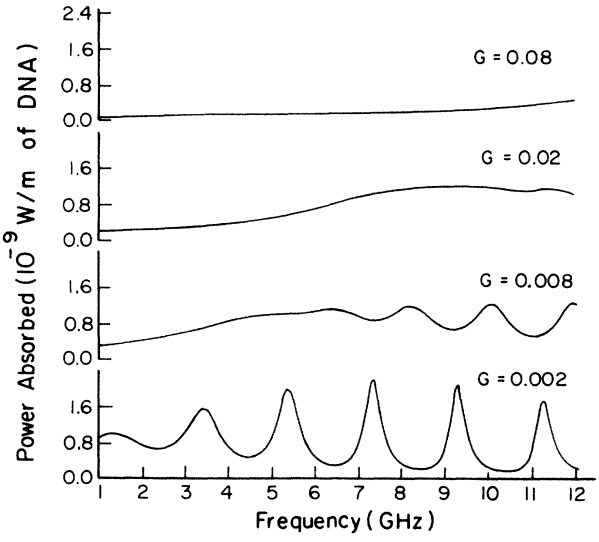


FIG. 5. Background subtracted power absorption spectra for various $G$ values at $\tau_1=0.039$ ns.

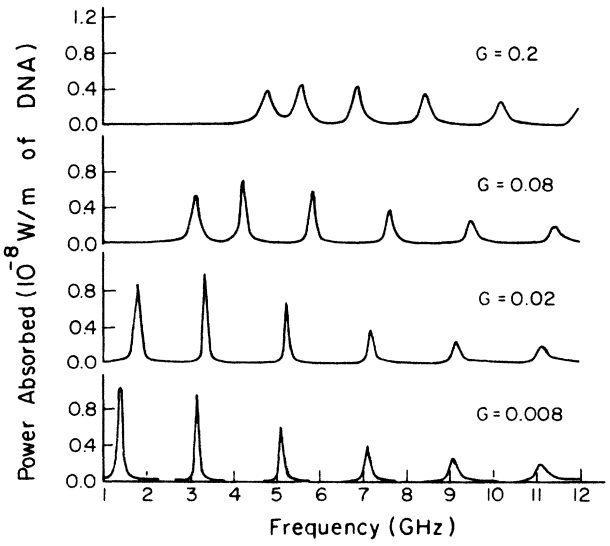


FIG. 7. Background subtracted power absorption spectra for various $G$ values at $\tau_1=1.000$ ns.

quoted by Edwards, Davis, Swicord, and Saffer. Of the runs we have shown, $G=0.02$ and $\tau_1=0.183$ ns compares "best" to the resonance positions, so we choose it to disect. (Note that due to the interrelated nature of $G$ and $\tau_1$ described above, other combinations, e.g., $G=0.004$ and $\tau_1=0.04$ ns, would also compare well.) In Figs. 8 and 9 we show the total absorption and how that absorption is distributed between the pieces of the model. A few interesting features can be seen in these figures. First note that the peak absorptions in the DNA molecule begin to fall away for higher modes even though these modes are driven with the same amplitude. In contrast, the resonant absorption by the continuum water seems to increase with the higher modes. Apparently the DNA works harder as a source for the higher modes, feeding more energy back into the reradiated fields.

The hydration layer absorption also shows interesting features. The dip in the power absorption below the first resonance results from the coupling to the molecule still being strong at this frequency. This allows the resonant motion of the DNA molecule to draw the hydration layer along with it causing the ions in the hydration layer to radiate more energy to the electric fields than it absorbs. Another interesting point can be seen by comparing the DNA and hydration layer absorptions. There is a shift between the lowest resonances in the hydration layer and the molecule itself. This corresponds to the different speed of sound in the hydration layer. This does not contribute to a significant broadening, however, because of the much smaller magnitude of the hydration layer absorption.

Some representative views of the fields themselves for the "best" parametrization are shown in Figs. 10–12 for $n=1$ at 1 GHz, $n=17$ at 1 GHz, and $n=1$ on resonance, respectively, where $n$ is the number of half-wavelengths on the 918-nm DNA molecule. The $n=1$ plots show the axial electric field dominated by the effectively constant driving field. The odd seeming increase in the $n=17$ axial electric field and all of the radial electric fields with radius is just the result of the loss to the solvent as the driving field propagates inward and the response field propagates outward. In a lossless medium the incoming and outgoing fields would cancel, and the radial electric field would vanish at large distances. It is notable also that the velocity and electric field disturbances remain significant for large distances away from the molecule.

The relative motion of the hydration layer and the

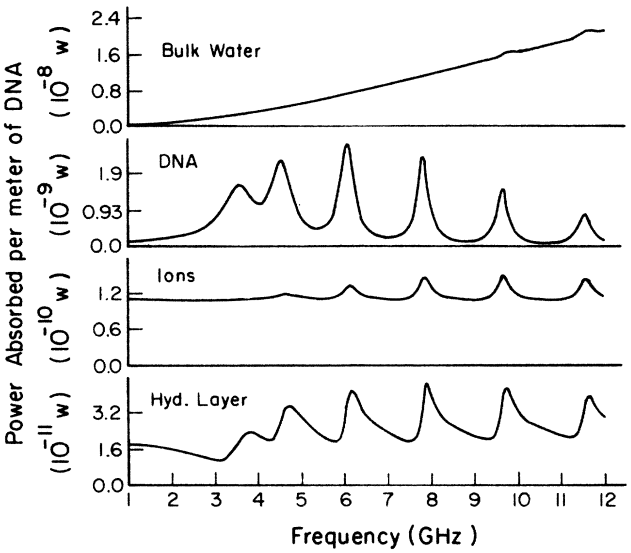


FIG. 9. Power absorption as it is distributed throughout the system. From top to bottom the spectra are for the continuum water, the DNA, the ions, and the hydration layer. Note the progression of scales.

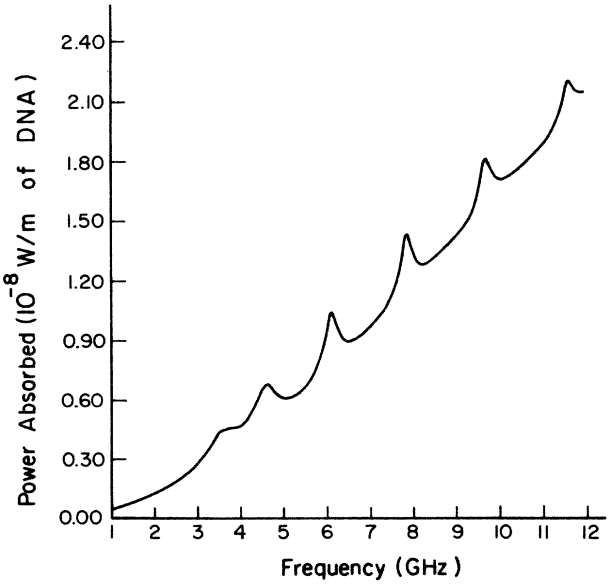


FIG. 8. Total power absorption per meter of DNA in a 0.1% volume DNA 5-mm NaCl solution.

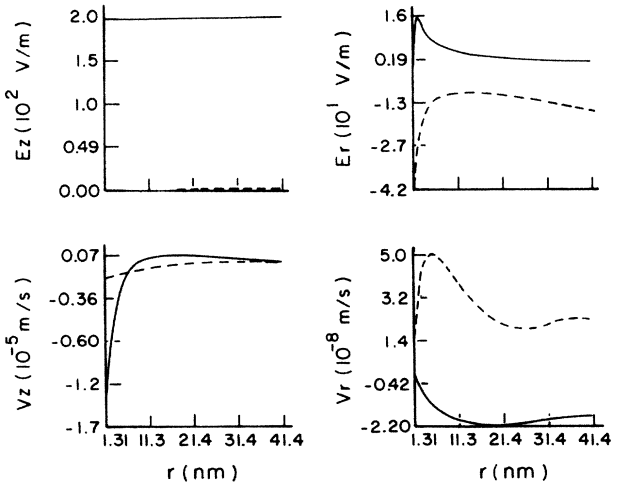


FIG. 10. Continuum fields vs radial distance from the DNA axis for the $n=1$ mode at 1 GHz. The solid and dashed lines are, respectively, the real and imaginary parts of each field.

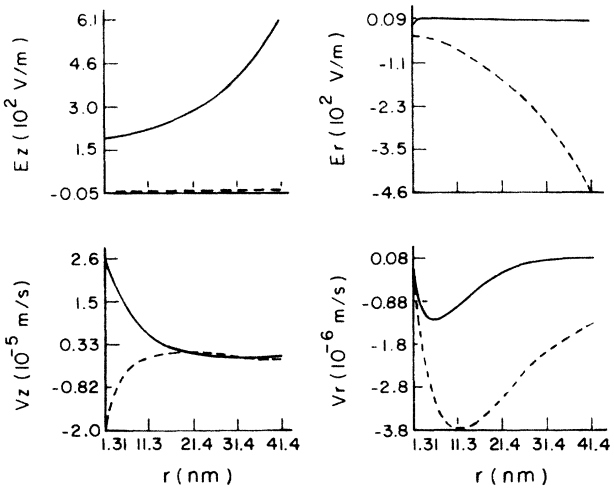


FIG. 11. Continuum fields vs radial distance from the DNA axis for the $n = 17$ mode at 1 GHz. The solid and dashed lines are, respectively, the real and imaginary parts of each field.

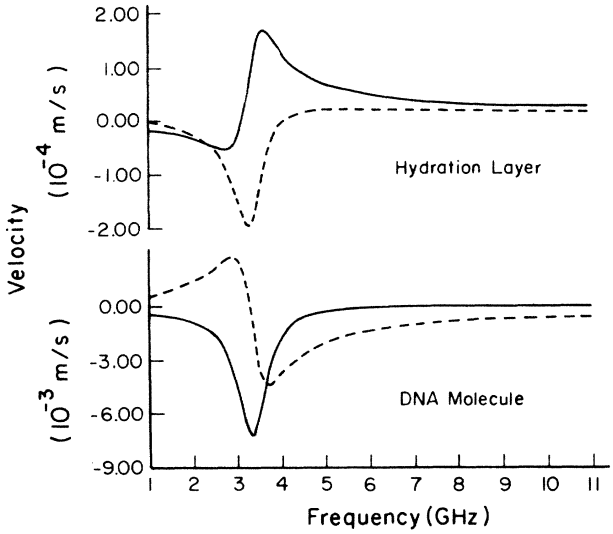


FIG. 13. Comparison of hydration layer (upper) and DNA (lower) velocities for the $n = 1$ mode as a function of frequency. The solid and dashed lines are, respectively, the real and imaginary parts of each field.

molecule for the $n = 1$ mode are diagramed in Fig. 13. The large difference between the motion of the hydration layer and the molecule is not surprising. As we observed in our previous paper, the no-slip condition requires the balancing of the damping force and the driving force, both of which must be large compared to the inertia and stiffness of the molecule. A small mismatch of these two forces can lead to very strongly decoupled motion. The small amplitudes of these motions, though, keeps this decoupling from disrupting the concept of a hydration layer, or our small amplitude approximations.

Taking this parametrization we are investigating the variations in the absorption with respect to salt concentration and temperature. These results will appear elsewhere.

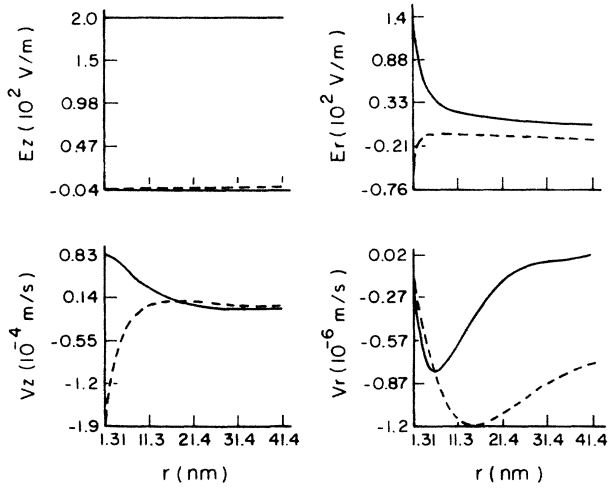


FIG. 12. Continuum fields vs radial distance from the DNA axis for the $n = 1$ mode on resonance. The solid and dashed lines are, respectively, the real and imaginary parts of each field.

## VI. CONCLUSIONS

This work is certainly not the final word on the subject of microwave absorption by DNA, since it only provides a framework for understanding where the anomalous behavior must be if the EDSS results are correct. Obviously, given free reign with the parameter $G$, it is easy to produce a power spectrum with resonances for any value of $\tau_1$. One need only decrease $G$ to eliminate enough damping to allow the molecule to move and leave enough to provide a loss mechanism. To get the proper positions and widths, however, requires a unique combination of $G$ and $\tau_1$ and the characteristic spacing of this parametrization.

Our results indicate that the EDSS results require a very strong orientational effect weakening the hydration layer's ability to transmit shearing forces to the molecule. A couple of simple considerations of such a situation takes us within a factor of 5 of the parameters needed to produce the EDSS results. This factor could show itself as a larger than measured relaxation time and/or a further reduction in $G$. As we mentioned, additional considerations, such as the length dependence of hydrogen bond strength and bond disruptions by the large counterion densities near the polymer, could easily close this gap. Whatever the case, it is this hydration layer that is of importance in this phenomenon. All other material properties play a role only inasmuch as they affect the hydration layer binding. Further study of the hydration layer on a molecular basis will be necessary to answer these questions and put our parametrization on a firmer theoretical footing.

*Present address: Department of Chemistry, University of Houston, University Park Campus, Houston, Texas 77004.

[1]G. Maret, R. Oldenbourg, D. Dransfeld, and A. Rupprecht, Colloid Polym. Sci. **257**, 1017 (1979).

[2]S. M. Lindsay and J. Powell, *Structure and Dynamics: Nucleic Acids and Proteins,* edited by E. Clementi and R. Sarma (Adenine, New York, 1983), pp-241–259.

[3]B. H. Dorfman and L. L. VanZandt, Biopolymers **22**, 2639 (1983).

[4]G. S. Edwards, C. C. Davis, J. D. Saffer, and M. L. Swicord, Phys. Rev. Lett. **53**, 1284 (1984).

[5]M. B. Hakim, S. M. Lindsay, and J. Powell, Biopolymers **23**, 1185 (1984).

[6]L. L. VanZandt and M. E. Davis, J. Biomol. Struct. Dyn. **2**, 1045 (1986).

[7]L. L. VanZandt, Phys. Rev. Lett. **57**, 2085 (1986).

[8]W. N. Mei, M. Kohli, E. W. Prohofsky, and L. L. VanZandt, Biopolymers **20**, 833 (1981).

[9]*American Institute of Physics Handbook,* 3rd ed., edited by D. E. Gray (McGraw-Hill, New York, 1972).

[10]D. Eisenberg and W. Kauzman, *The Structure and Properties of Water* (Oxford University Press, London, 1969).

[11]A. R. Dexter and A. J. Matheson, Adv. Mol. Relaxation Processes **2**, 251 (1972).

[12]N. J. Tao, S. M. Lindsay, and A. Rupprecht, Biopolymers **26**, 171 (1987).

[13]M. L. Kopka, A. V. Fratini, H. R. Drew, and R. E. Dickerson, J. Mol. Biol. **163**, 129 (1983).

[14]E. R. Lippincott and R. Schroeder, J. Chem. Phys. **23**, 1099 (1955).

[15]M. Fixman, J. Chem. Phys. **70**, 4995 (1979).

[16]W. H. Press, B. P. Flannery, S. A. Teukolsky, and W. T. Vetterling, *Numerical Recipes: The Art of Scientific Computing* (Cambridge University Press, Cambridge, England, 1986).

[17]M. LeBret and B. H. Zimm, Biopolymers **23**, 287 (1984).